Electronic Supplementary Material (ESI) for Journal of Materials Chemistry A.

Supporting Information

Insight into the topological defects and dopants in metal-free holey graphene for triiodide reduction in dye-sensitized solar cells

Wang Yang[a], Xiuwen Xu[a], Liqiang Hou[a], Xinlong Ma[a], Fan Yang[a], Ying Wang[b*] and Yongfeng Li[a*]

[a]*State Key Laboratory of Heavy Oil Processing, China University of Petroleum, Beijing Changping 102249, China*

[b]*State Key Laboratory of Rare Earth Resource Utilization, Changchun Institute of Applied Chemistry, Chinese Academy of Sciences, Changchun 130022, China*

*Corresponding author.

E-mail: ywang_2012@ciac.ac.cn (Y. Wang); yfli@cup.edu.cn (Y. Li)

Experimental Section

Nitrogen-doped graphene (NG) fabrication: Graphene oxide (GO) was prepared from natural graphite powder (Sigma, 325 mesh) by a modified Hummer's method. Pre-oxidation of graphite was carried out as reported by Kovtyukhova et al.,[1] followed by oxidation using the Hummer's method.[2] Then nitrogen-doped graphene (NG) was fabricated from the GO precursor. The GO powder was firstly dispersed in deionized water to obtain a homogeneous GO aqueous dispersion (2.0 mg mL^{-1}). Then, urea was added into the GO dispersion with a GO to urea weight ratio of 1:15 to serve as the nitrogen source. The prepared dispersion was then put into a 100.0 mL Teflon autoclave and hydrothermally treated at 180 ^{o}C for 18.0 h. After hydrothermal treatment, washing, filtering, and freeze-drying, and thus we obtained the NG.

Table S1 Atomic concentration of C, N, and O of HG, NHG-1 and NHG-2.

Sample	C (at%)	N (at%)	O (at%)
HG	97.65	0	2.35
NHG-1	96.39	1.09	2.52
NHG-2	94.13	2.85	3.02

Table S2 Performance of nitrogen-doped nanocarbon-based CEs in DSSCs reported in recent literatures (based on I^-/I_3^- redox couple)

Sample	N content	Thickness (μm)	S_{BET} (m^2 g^{-1})	PCE (%)	PCE_{Pt} (%)	PCE/ PCE_{Pt}	Reference
Nitrogen-doped graphene (GO)	7.4 at%	-	-	5.4	5.1	1.058	1[3]
Nitrogen-doped graphene (GO)	-	-	-	4.75	5.03	0.944	2[4]
Nitrogen-doped graphene nanosheets	-	32	-	7.18	7.58	0.947	3[5]
Nitrogen-doped graphene (GO)	2.96 at%	-	130	5.89	7.58	0.777	4[6]
Nitrogen-doped graphene foams	7.6 at%	30	436	7.07	7.44	0.950	5[7]
p-Doped three-dimensional graphene	0.5 wt%	-	1025	8.46	7.98	1.060	6[8]
Nitrogen-doped CVD graphene film	4.38 at%	-	-	3.12	6.93	0.450	7[9]
Nitrogen-doped graphene nanoribbons	2.80 wt%	-	325	8.57	7.84	1.093	8[10]
Nitrogen-doped graphene	2.5 at%	-	289	7.01	7.34	1.047	9[11]
Nitrogen doped porous graphene	9.39 at%	-	163.7	6.8	7.0	0.971	10[12]
Nitrogen doped holey rGO	5.2 at%	-	305.8	5.56	5.45	1.02	11[13]
Nitrogen-doped graphene nanosheets	5.79 at%	-	-	8.71	9.93	0.877	12[14]
N-doped GO (NG) aerogels	2.32 at%	-	13	5.14	7.16	0.717	13[15]
Nitrogen-doped graphene sheets (N-rGO)	2.5 at%	-	-	6.12	6.97	0.878	14[16]
N-doped porous graphene foams	11.65% (N/C)	-	479	4.5	4.9	0.918	15[17]

Edge-nitrogenated graphene nanoplatelets	-	3.5	679	7.69	8.06	0.954	16[18]
Nitrogen doping reduced graphene oxide	7.31 at%	-	-	8.03	7.33	1.09	17[19]
Nitrogen-doped mesoporous carbon	4 at%	6.53	637	7.02	7.26	0.967	18[20]
N‑doped hierarchical hollow mesoporous carbon	4.05 at%		1743	6.38	7.19	0.887	19[21]
Nitrogen-doped ordered cubic mesoporous carbons	1.54 at%	-	642	5.60	6.46	0.853	20[22]
N-doped macro/mesoporous carbon	5.3 at%	-	728	7.27	6.92	1.05	21[23]
N-doped carbon nanotube arrays	3.76 at%	20	-	7.04	7.34	0.959	22[24]
Nitrogen-doped carbon nanotube-based bilayer thin film	-	40 nm	-	1.53	3.95	0.387	23[25]
N-doped graphene-CNT	-	-	-	6.74	6.89	0.978	24[26]
N-doped holey graphene	**2.85 at%**	**4.3**	**1874**	**9.07**	**8.19**	**1.108**	**Our work**

Table S3 Photovoltaic parameters of DSSCs with Ar-HG, NG and NHG-2 CEs under 1 sun illumination (AM 1.5) and the simulated data from EIS

CE	I_{sc} (mA/cm^2)	V_{oc} (V)	FF	PCE (%)	R_s (Ω cm^2)	R_{ct} (Ω cm^2)	Z_{pore} (Ω cm^2)
Ar-HG	16.64	0.736	0.658	8.06	5.04	2.96	0.73
NG	15.47	0.736	0.596	6.78	6.69	5.25	0.64
NHG-2	17.19	0.744	0.709	9.07	5.03	1.92	0.62

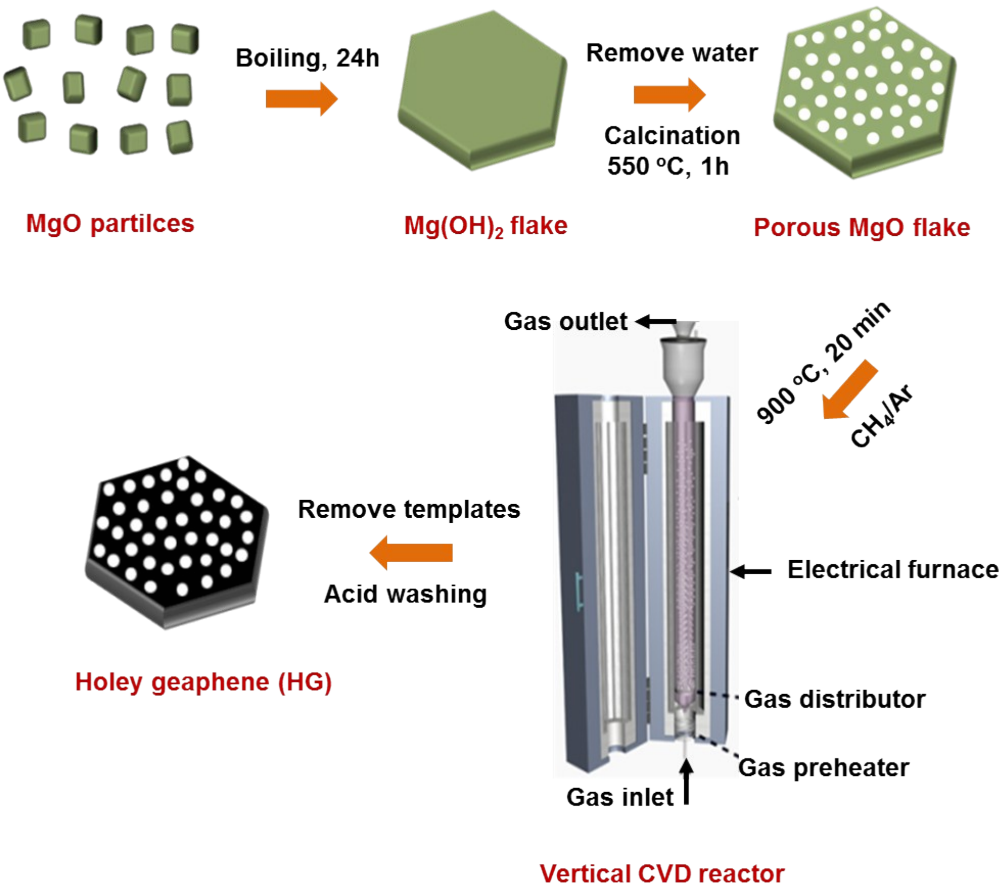

Fig. S1. Schematic illustration of preparation process of holey graphene (HG).

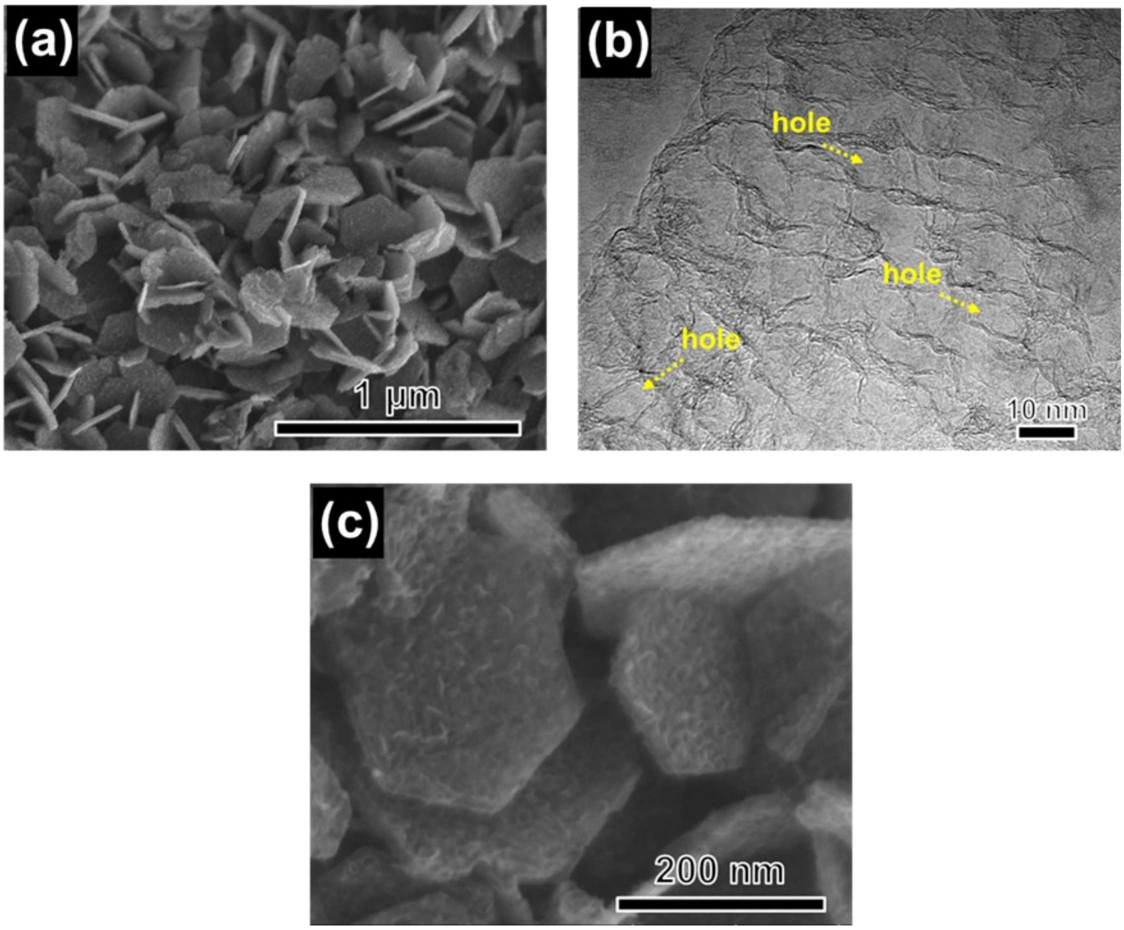

Fig. S2. SEM (a) and TEM (b) images of pristine HG. c) A SEM image of NHG.

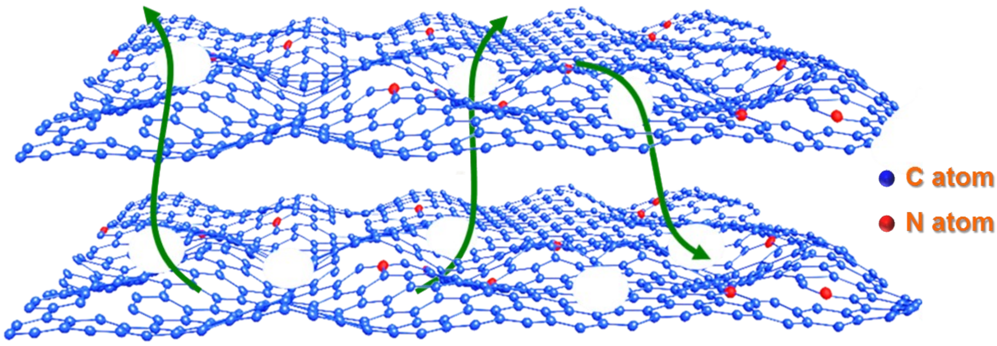

Fig. S3. The schematic illustration of the ion-diffusion pathway across the hole.

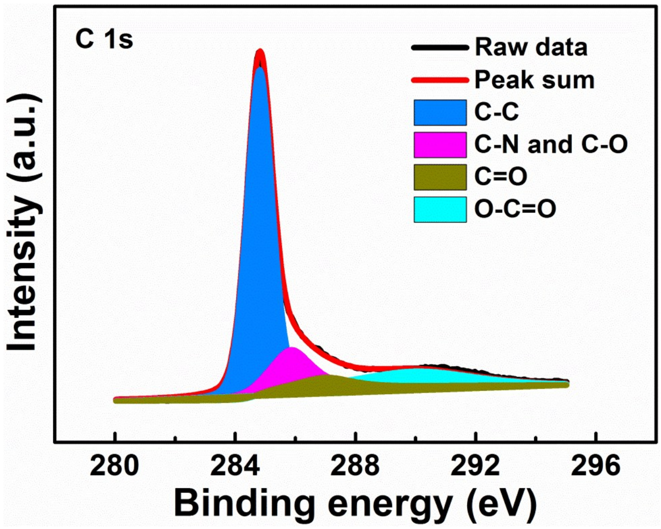

Fig. S4. A high resolution spectra of C1s for NHG-2.

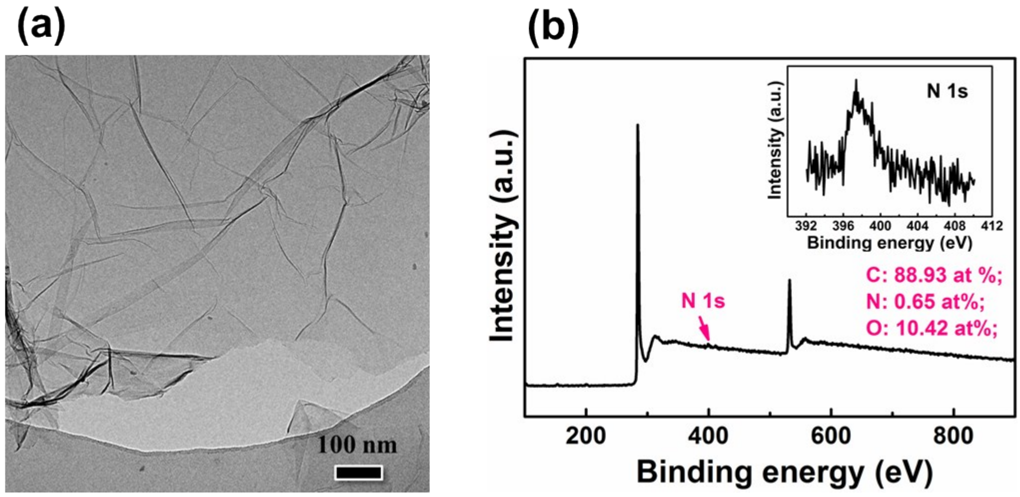

Fig. S5. (a) A TEM image of N-rGO, showing few in-plane edges in the graphene layers. (b) The XPS survey of N-rGO and the high resolution spectra of N1s (inset).

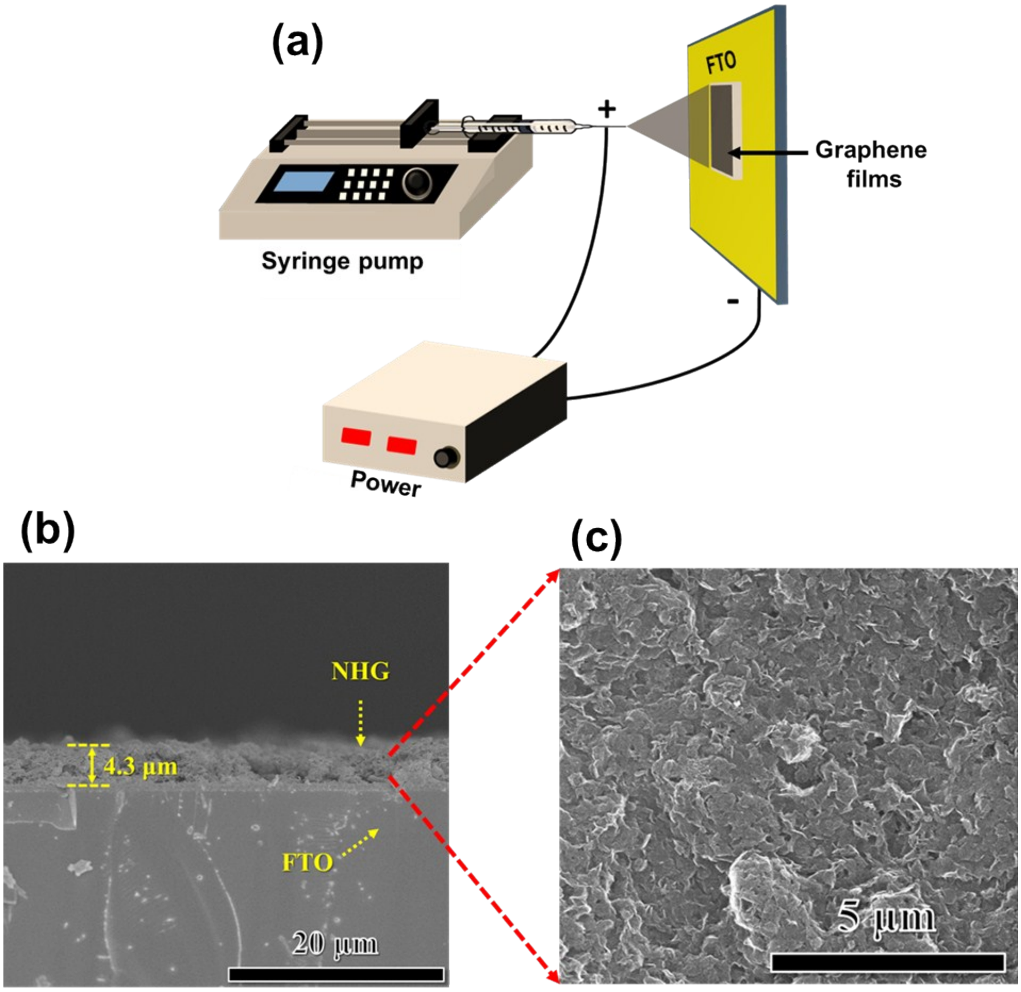

Fig. S6. A schematic diagram of the e-spray setup used for NHG counter electrode film fabrication (a) and SEM images of NHG CEs on FTO substrates (b, c).

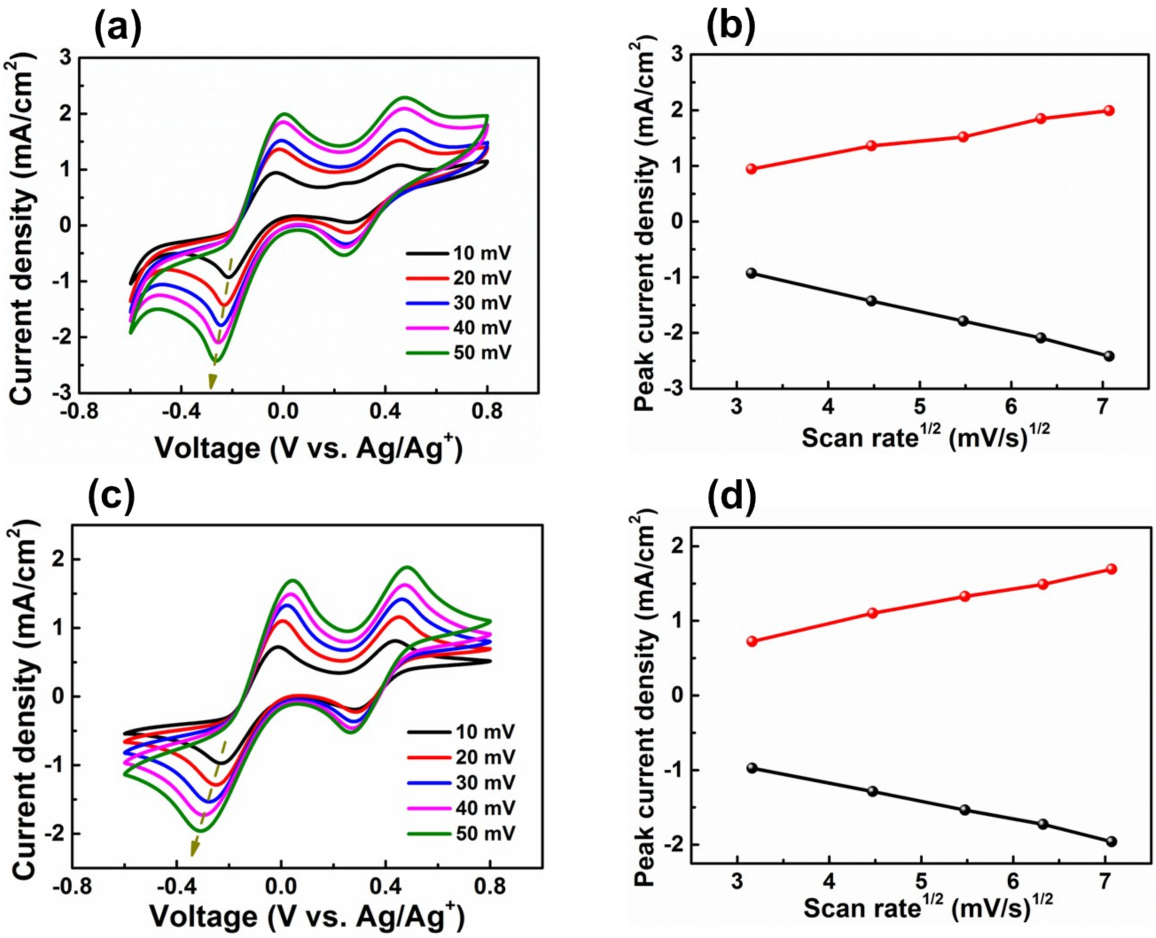

Fig. S7. Cyclic voltammograms curves of (a) NHG-2 electrode and (c) Pt electrode at various scanning rates (10, 20, 30, 40, and 50 mV/s), respectively. The peak current density of the left peak pairs as a function of the square root of the scan rates for NHG-2 (b) and Pt (d) electrode, respectively.

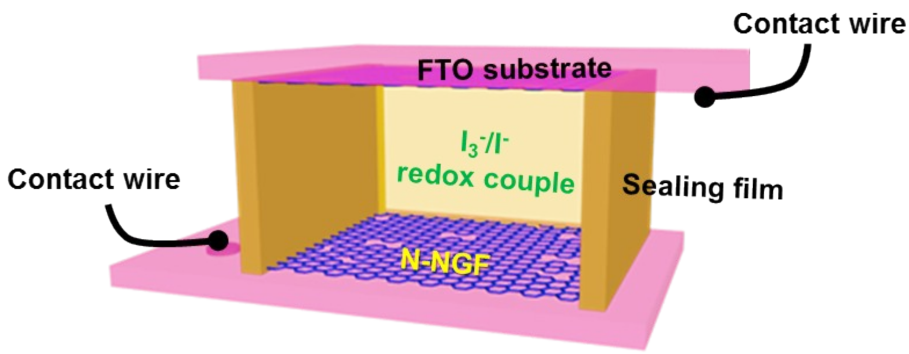

Fig. S8. Schematic structure of a symmetric cell symmetrical dummy cell using two identical electrodes.

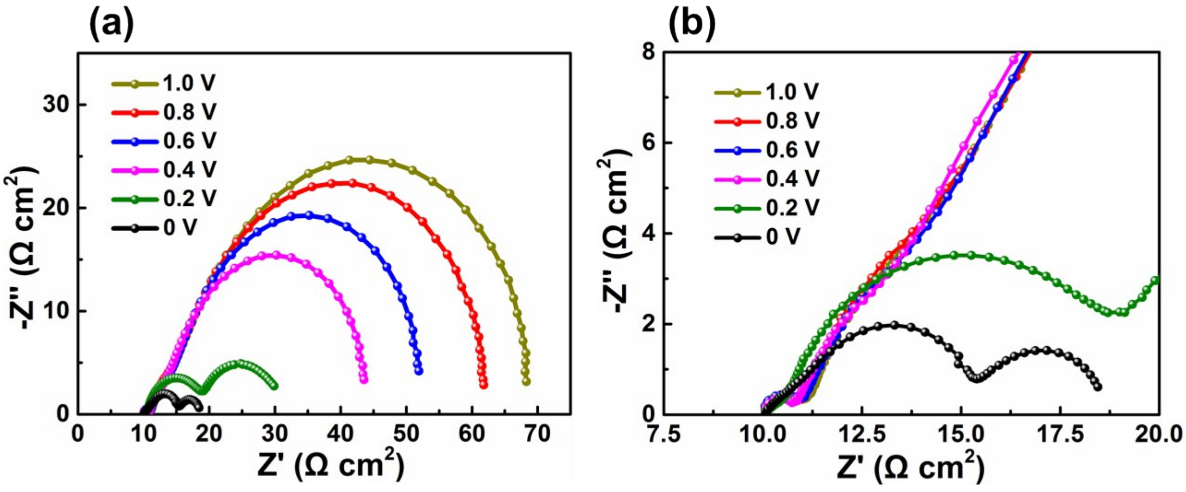

Fig. S9. (a) Nyquist plots of impedance spectra on symmetrical dummy cell with NHG-2 electrode at various applied biases. (b) An expansion of the high frequency region. The legend in (b) is for (a) as well.

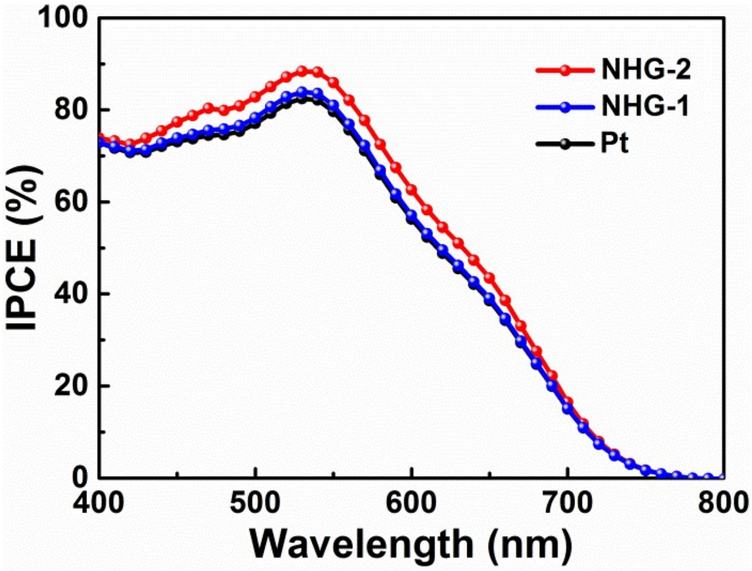

Fig. S10. IPCE spectra for DSSCs with NHG and Pt CEs.

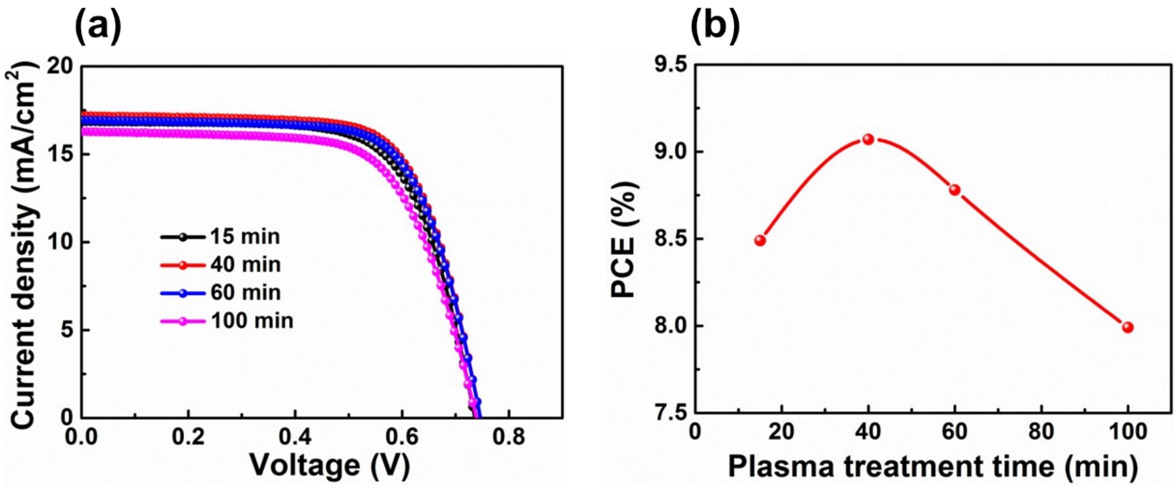

Fig. S11. (a) Current-voltage characteristics of the DSSCs based on NHG electrodes with different plasma treatment time. (b) Plot of the PCE versus N2 plasma treatment time.

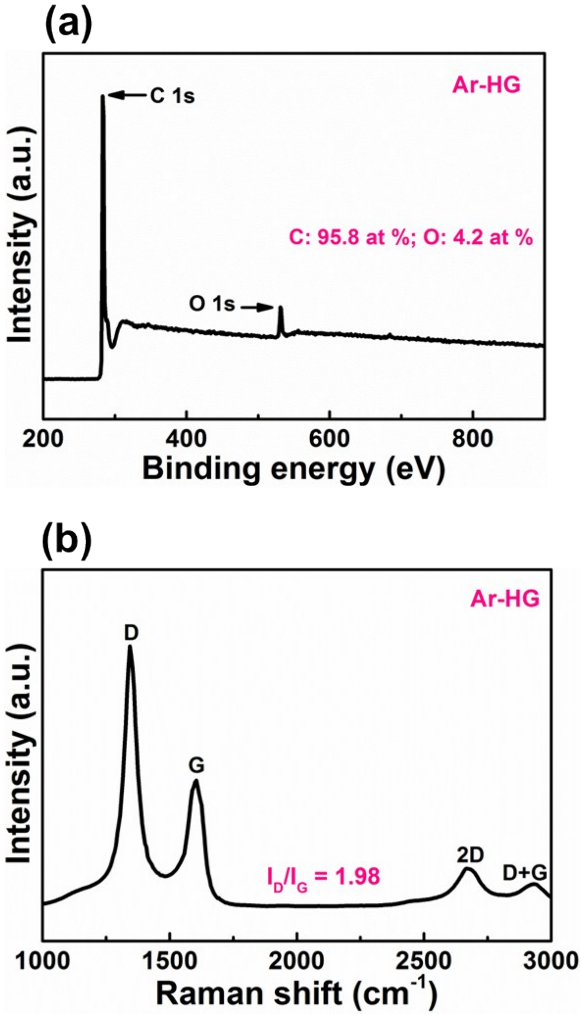

Fig. S12. (a) XPS survey of Ar-HG. (b) Raman spectra of Ar-HG.

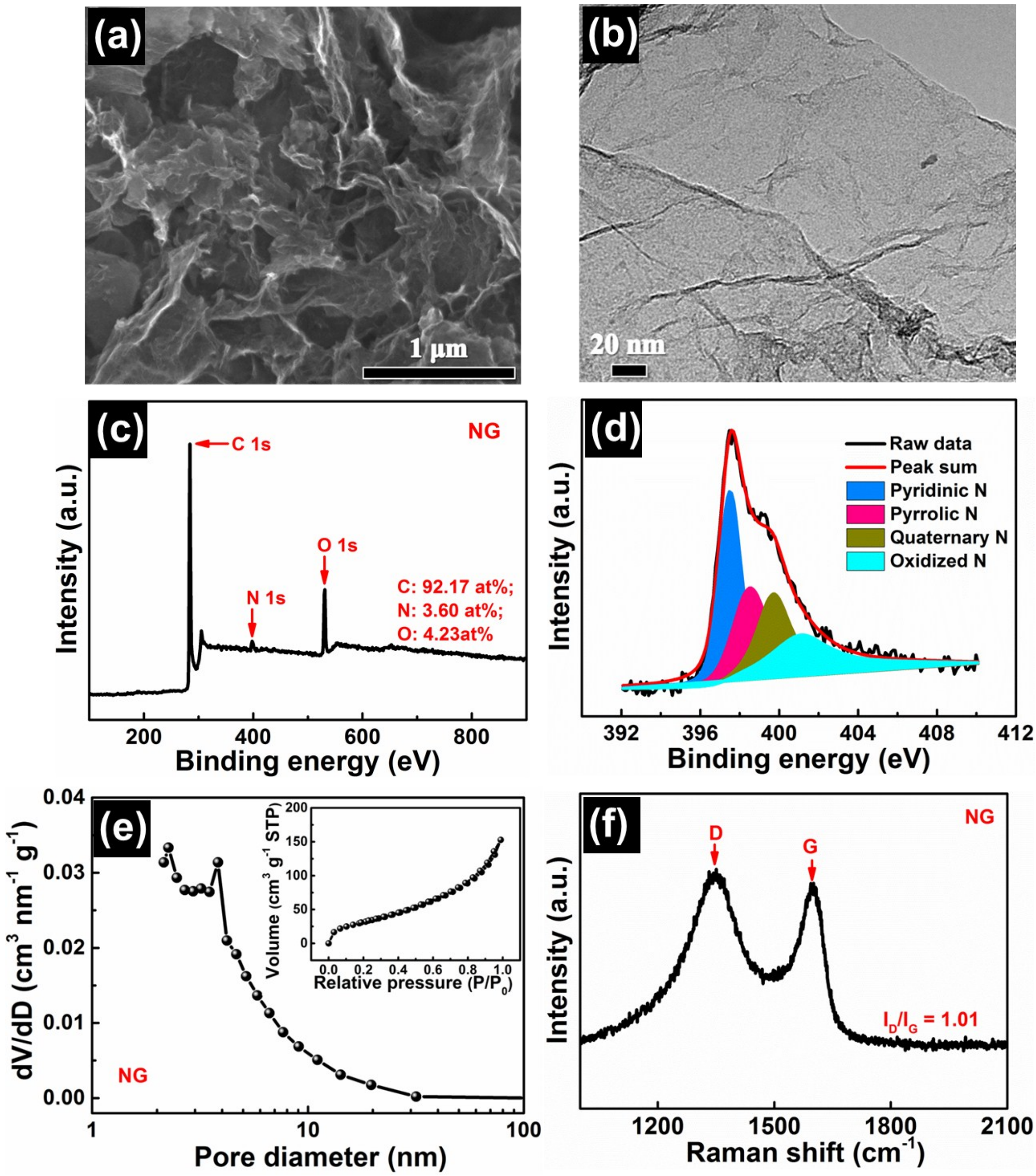

Fig. S13. (a) SEM and (b) TEM images of NG, showing few in-plane holes in the graphene layers. (c) The XPS survey of NG. (d) The high-resolution N1s XPS spectrum of NG. (e) The N_2 sorption isotherms and pore size distribution of NG (inset). (f) Raman spectra of NG.

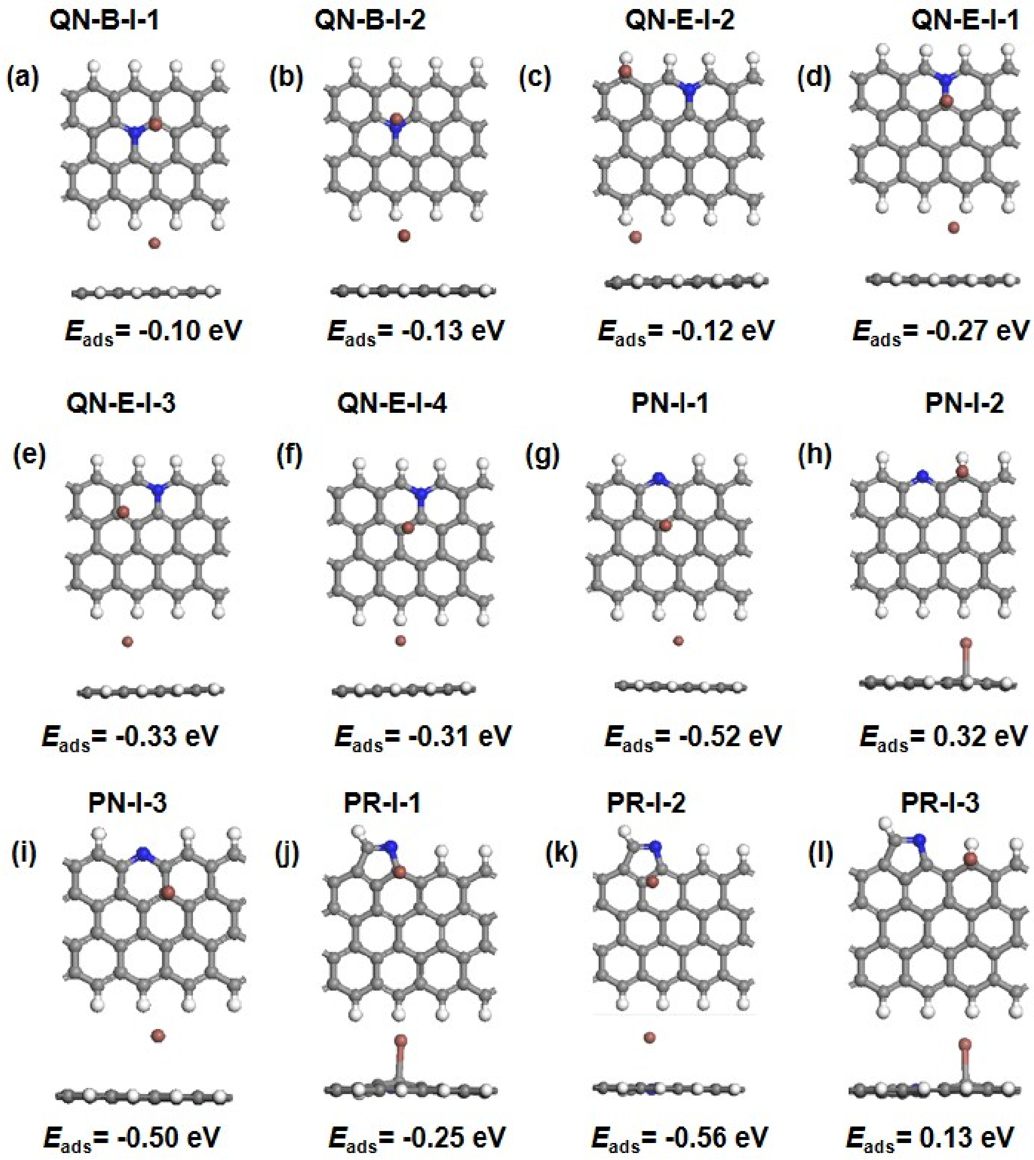

Fig. S14. The other investigated structures of I atom adsorption on (a,b) QN-B; (c-f) QN-E); (g-i) PN; (j-l) PR, as well as the adsorption energy of I atom (E_{ads}).The gray, blue, brown and white balls stand for C, N, I, and H atoms, respectively.

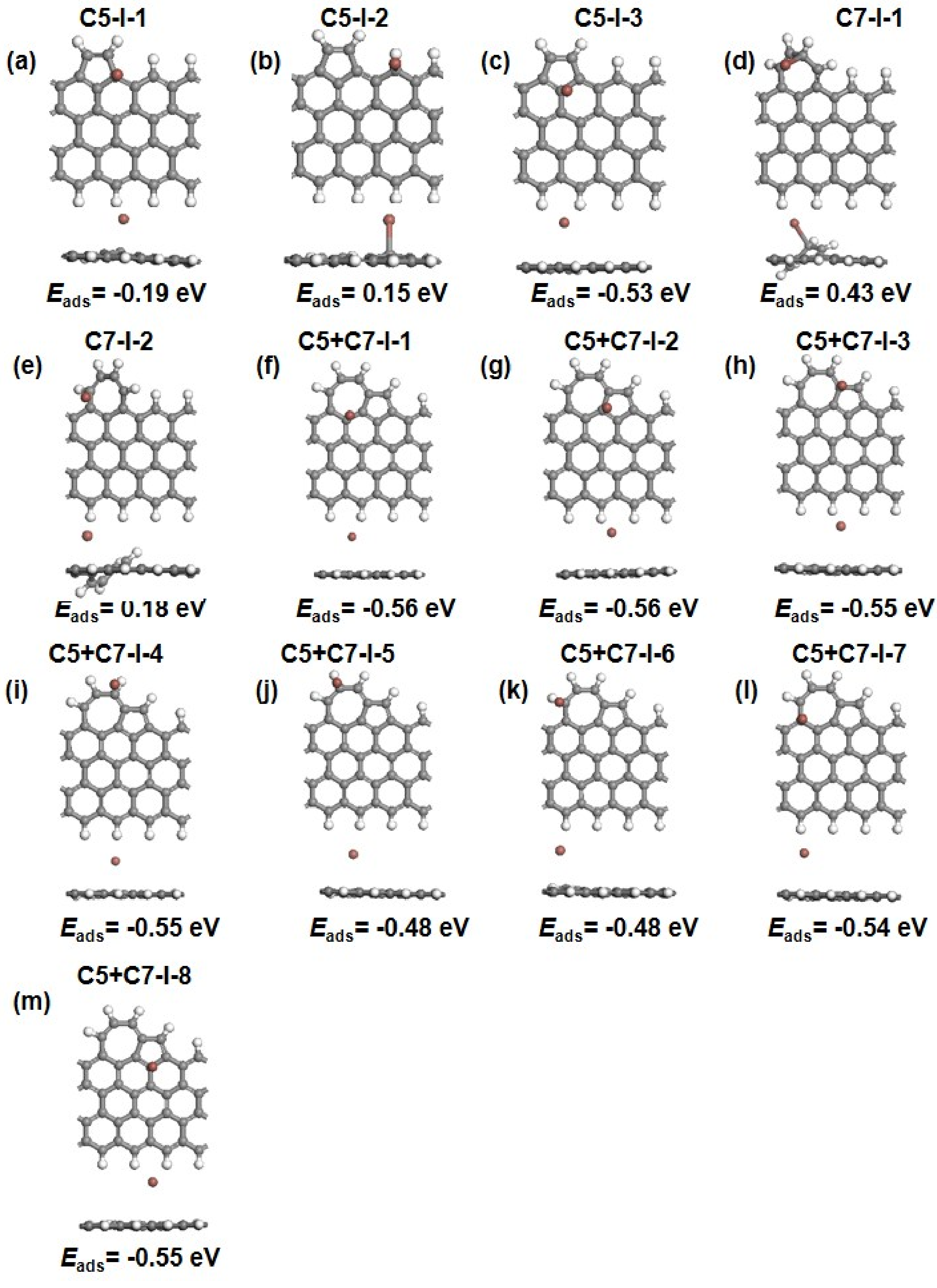

Fig. S15. The other investigated structures of I atom adsorption on (a-c) C5; (d, e) C7; (f-m) C5+C7 as well as the adsorption energy of I atom (E_{ads}). The gray, blue, brown and white balls stand for C, N, I, and H atoms, respectively.

References

[1] N. I. Kovtyukhova, P. J. Ollivier, B. R. Martin, T. E. Mallouk, S. A. Chizhik, E. V. Buzaneva, *Chem. Mater.*, 1999, **11**, 771-779.

[2] J. W. Hummers, R. E. Offeman, *J. Am. Chem. Soc.*, 1958, **80**, 1339-1342

[3] S. Hou, X. Cai, H. Wu, X. Yu, M. Peng, K. Yan, D. Zou, *Energy Environ. Sci.*, 2013, **6**, 3356-3362.

[4] M. Y. Yen, C. K. Hsieh, C. C. Teng, M. . Hsiao, P. . Liu, C. . M. Ma, M. . Tsai, C. Tsai, Y. Lin, T. Chou, *RSC Adv.*, 2012, **2**, 2725-2728.

[5] P. Zhai, T. C. Wei, Y. H. Chang, Y. T. Huang, W. T. Yeh, H. Su, S. P. Feng, *Small*, 2014, **10**, 3347-3353.

[6] A. G. Kannan, J. Zhao, S. G. Jo, Y. S. Kang, D. W. Kim, *J. Mater. Chem. A*, 2014, **2**, 12232-12239.

[7] Y. Xue, J. Liu, H. Chen, R. Wang, D. Li, J. Qu, L. Dai, *Angew. Chem. Int. Ed.*, 2012, **51**, 12124-12127.

[8] H. J. Ahn, I. H. Kim, J. C. Yoon, S. I. Kim, J. H. Jang, *Chem. Commun.*, 2014, **50**, 2412-2415.

[9] W. Yang, X. Xu, Z. Tu, Z. Li, B. You, Y. Li, S. I. Raj, F. Yang, L. Zhang, S. Chen, *Electrochim. Acta*, 2015, **173**, 715-720.

[10] X. Meng, C. Yu, X. Song, Y. Liu, S. Liang, Z. Liu, C. Hao, J. Qiu, *Adv. Energy Mater.*, 2015, **5**, 1500180-1500189.

[11] G. Wang, W. Xing, S. Zhuo, *Electrochim. Acta*, 2013, **92**, 269-275.

[12] Z. Gao, L. Wang, J. Chang, X. Liu, D. Wu, F. Xu, Y. Guo, K. Jiang, *Electrochim. Acta*, 2016, **188**, 441-449.

[13] M. Yu, J. Zhang, S. Li, Y. Meng, J. Liu, *J. Power Sources*, 2016, **308**, 44-51.

[14] J. Balamurugan, T. D. Thanh, N. H. Kim, J. H. Lee, *Adv. Mater. Inter.*, 2016, **3**

[15] J. Ma, C. Li, F. Yu, J. Chen, *ChemSusChem*, 2014, **7**, 3304-3311.

[16] G. Wang, Y. Fang, Y. Lin, W. Xing, S. Zhuo, *Mater. Res. Bull.*, 2012, **47**, 4252-4256.

[17] L. Song, Q. Luo, F. Zhao, Y. Li, H. Lin, L. Qu, Z. Zhang, *Phys. Chem. Chem. Phys.*, 2014, **16**, 21820-21826.

[18] G. Wang, J. Zhang, S. Hou, W. Zhang, Z. Zhao, *Nanoscale*, 2016, **8**, 9676-9681.

[19] X. Zhang, S. Pang, X. Chen, K. Zhang, Z. Liu, X. Zhou, G. Cui, *RSC Adv.*, 2013, **3**, 9005-9010.

[20] G. Wang, S. Kuang, D. Wang, S. Zhuo, *Electrochim. Acta*, 2013, **113**, 346-353.

[21] D. S. Yang, C. Kim, M. Y. Song, H. Y. Park, J. C. Kim, J. J. Lee, M. J. Ju, J. S. Yu, *J. Phys. Chem. C*, 2014, **118**, 16694-16702.

[22] M. Chen, L. L. Shao, Y. P. Liu, T. Z. Ren, Z. Y. Yuan, *J. Power Sources*, 2015, **283**, 305-313.

[23] L. Li, C. L. Wang, J. Y. Liao, A. Manthiram, *J. Power Sources*, 2015, **300**, 254-260.

[24] K. S. Lee, W. J. Lee, N. G. Park, S. O. Kim, J. H. Park, *Chem. Commun.*, 2011, **47**, 4264-4266.

25] H. Tantang, A. K. K. Kyaw, Y. Zhao, M. B. Chan, A. I. Y. Tok, Z. Hu, L. J. Li, X. W. Sun, Q. Zhang, *Chem.-Asian J.*, 2012, **7**, 541-545.

[26] J. Ma, C. Li, F. Yu, J. Chen, *J. Power Sources*, 2015, **273**, 1048-1055.